

Experimental and Numerical Fluid Flow Study on a X-Millichannel

C. Wolluschek^{*1}, F. Etcheverry², M. Cachile², J. Gomba³

¹Mecánica de Fluidos e Ingeniería Térmica, Centro tecnológico Cemitec, España, ²Grupo de Medios Porosos, Facultad de Ingeniería, UBA, Argentina, ³Instituto de Física Arroyo Seco, UNCPBA, Tandil, Argentina.

*cwollus@cemitec.com

Abstract: In this work a model that predicts velocity and concentration fields inside an X-shaped millichannel (4 mm diameter) is developed. Water and a low concentration ink are injected simultaneously in the two inlets of the device. The mass transfer problem is solved by a Fickian model (solute concentration is low compared with the solvent). The key idea is to understand the role of diffusion and the velocity field in the flow mixture. The numerical results are compared with the experimental ones.

Keywords: porous media, millichannel, pasive millimixer, diffusion.

1. Introduction

The aim of this paper is to study, experimentally and numerically, millimeter flows that simulate flow patterns in a pore of a porous medium. The millichannels and cavities studied in this work will allow exploring and quantifying the importance of the various types of interactions: diffusion, geometric scattering, effect of the wall roughness, etc. The porous media are present in many branches of science and technology such as oil recovery from petroleum reservoirs, pharmaceutical industry, geology, biology, etc. One of the effects of the porous media on flows, is to produce dispersion, due to the different paths to travel inside the matrix, even at low Reynolds numbers [1,2]. For this reason, in many applications, it is possible to consider the porous media as a system of highly interconnected capillaries networks [3,4]. Usually, the behavior of a porous media is studied on a macroscopic scale, i.e. at the complete medium level. However, the study presented here proposes an analysis starting from the microscopic scale (pore-level), through the study of mixing properties depending on the geometry.

As a first step, we induce millimeter interactions by intersecting channels, in order to characterize the geometric problem and to identify the relevant parameters.

In particular, we study two cross-millichannels with two inlets and two outlets. By injecting a colored dispersion in one of the inlets and distilled water in the other, we compared the outlet concentrations from experimental and numerical models. In order to improve our understanding of the problem and to perform parameter variations in future phases of this work, the problem has been modeled in COMSOL 3.5.

2. Experiments

With the aim of study the properties of the mixing millimeter channels, we designed an experiment with two circular acrylic 4 mm internal diameter channels that intersect at an angle of 90 degrees. In one of the channels, a methylene blue ink (a water-based ink) at low concentration ($c = 1 \text{ mol/m}^3$) is injected. The ink diffusion coefficient is $D = 6.5 \cdot 10^{-10} \text{ m}^2/\text{s}$. In the second channel, distilled water ($c = 0 \text{ mol/m}^3$) is injected. The flow Q through both channels can be varied. The comparison between numerical simulations and experiments has been done for $Q = 0.006 \text{ l/min}$. The channels were made of transparent material to visualize the ink concentration distribution with an optical system specially prepared for this purpose.

3. Use of COMSOL Multiphysics

3.1 Model overview

The fluid flow is described by the laminar steady-state Navier-Stokes and continuity equations:

$$\rho \frac{\partial u}{\partial t} - \nabla \cdot \eta(\nabla u + (\nabla u)^T) + \rho(u \cdot \nabla)u + \nabla p = 0 \quad [1]$$

$$\nabla \cdot u = 0 \quad [2]$$

where ρ represents the density (kg/m^3), \mathbf{u} the velocity (m/s), η the viscosity (N.s/m^2) and p the pressure (Pa). The considered fluid is water with a $\eta = 1\text{e-}3 \text{ N.s/m}^2$ and $\rho = 1\text{e}3 \text{ kg/m}^3$.

The mass balance equation is given by the convection-diffusion application mode and the equation to solve is:

$$\frac{\partial c}{\partial t} = -\nabla \cdot (-D\nabla c) - \mathbf{u} \cdot \nabla c = 0 \quad [3]$$

where D represents the diffusion coefficient and c gives the ink concentration. The boundary conditions at the inlets are $c = 1 \text{ mol/m}^3$ and $c = 0 \text{ mol/m}^3$. Due to this concentration value, we work with a low concentration system. This means that the solute molecules only interact with water molecules (without interacting with themselves) and thus, it is possible to use Fick' law to describe the diffusion process. Also, we assume that the concentration employed does not modify the density or viscosity of the water. Under these assumptions, it is legitimate to first solve the Navier-Stokes equations at steady state and then use its solution as a base flow to solve the non steady convection-diffusion equation.

3.3 Geometry

The 3D geometry used is shown in figure 1. The length of the channels is 1 cm. In order to simplify the simulation and exploiting the symmetry of the problem, we have studied only one of the horizontal planes.

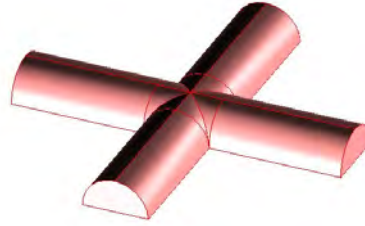
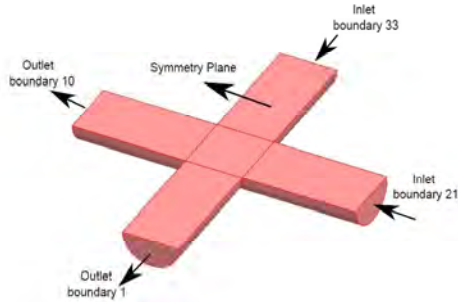


Figure 1: Sketch of the 3D geometry

For meshing geometry, we have used tetrahedral elements with different size at each interest volume. The maximum elements size are $5\text{e-}4 \text{ m}$ at the intersection volume and $8\text{e-}4 \text{ m}$ at the outlets channels. The inlet volumes have the default size (figure 2).

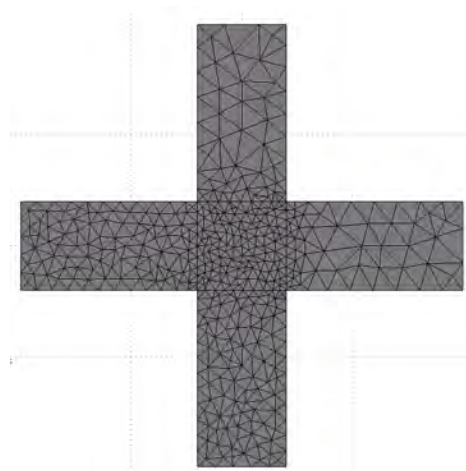


Figure 2: Sketch of the size elements in each interest volumes.

In total, we have a mesh of about 10600 finite elements, which corresponds to approximately 68100 degrees of freedom. As solver we have chosen the direct PARDISO. For the diffusion equations, different stabilization options has been tested since solutions not always were converged or were unstable ones.

3.2 Boundary conditions

At the inlets, the model assumes laminar fully developed flow. A parabolic velocity profile with a constant mass flow has been set

up. In the case of our study $Q = 0.006$ l/min has been used.

At the outlet, the pressure is set at 0 Pa. At the other boundaries, which are the external limits of the fluid, a non-slip condition is employed. Boundaries from the center horizontal plane are symmetry boundary.

3.4 Parameters

In the next table, parameters are indicated:

Flow inlet boundary #21	0.006 l/min
Flow inlet boundary #33	0.006 l/min
Concentration inlet #21	1 mol/m ³
Concentration inlet #33	0 mol/m ³

4. Model results

4.1 Hydrodynamic Model

The Reynolds number has been checked to be in the laminar regime in order to ensure that a laminar steady-state assumption is correct to study the present problem ($Re = 40$ in the simulated case).

The Navier-Stokes equations were solved, and figures 3 and 4 show the results of the velocity field.

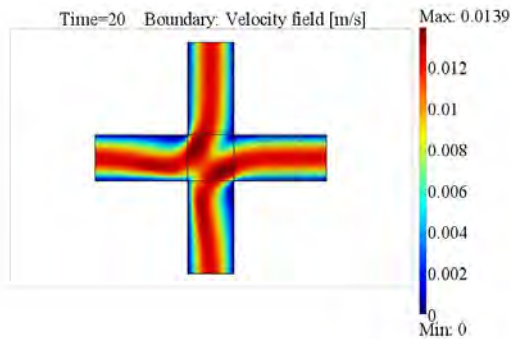


Figure 3: Modulus of the velocity vector.

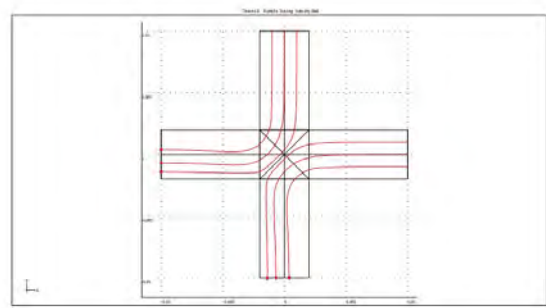


Figure 4: Streamlines

Related to the flow distribution, figure 3 shows that in the case with the same flow rate at two inlets, the flow is symmetric with respect to a bisecting plane, that is not crossed by the streamlines, as shown in figure 4.

Notice that the velocity is increased from 0.01 m/s at the inlet pipes to 0.0139 m/s at the central zone. The increments of the velocity corresponds to a section narrowing that occurs in the central zone. Effectively, the ratio between these two velocities is about 0,7 which is the ratio between the cross section of the inlet pipes and the ellipse at the bisecting plane.

4.2 Diffusion process

A brief preliminary study was conducted in order to explore some of the diffusion parameters available in COMSOL. By using the stationary solutions of the Navier-Sokes equations as a base state, we have studied the transient diffusion starting at the moment the ink enters the corresponding boundary ($c = 1$ mol/m³, boundary #21) until $c(r,t)$ reaches a stationary solution.

In order to detect when the stationary state for c is reached, not only the evolution of c along the channels but also the mean concentration \bar{c} at the exits are monitored, which is defined as

$$\bar{c}_i = \frac{1}{A} \iint_A c \, dA \quad [4]$$

Here A is the cross sectional area at the exit and the sub-index i stands for the exit boundaries, #1 or #10 (see figure 1). The quantity \bar{c} is a useful

control parameter, because the theory predicts that for $D \rightarrow 0$, $\bar{c}_1 \rightarrow 1 \text{ mol/m}^3$ and $\bar{c}_{10} \rightarrow 0 \text{ mol/m}^3$. On the other hand, when $D \rightarrow \infty$, $\bar{c}_1 = \bar{c}_{10} \rightarrow 0.5 \text{ mol/m}^3$.

Thus, these two limits will be important to evaluate the reliability of the numerical solutions.

Before showing the results of this section, we briefly describe the diffusion parameters [5].

Isotropic Diffusion. With this option, COMSOL adds a new term to the physical diffusion coefficient. The effect of isotropic diffusion is to damp oscillations and also avoid their propagation [5]. The tuning parameter, δ_{id} , controls the amount of the isotropic diffusion and should be as low as possible, usually lower than 0.5.

Streamline Diffusion. Streamline Diffusion is a direct refinement of the isotropic diffusion method described above. The main difference with the Isotropic Diffusion is that the Streamline Diffusion adds diffusion only in the streamline direction. Again, the value of the streamline diffusion, δ_{sd} , should be kept as low as possible (the default value is 0.25). COMSOL offers three different methods to introduce this diffusion: the Anisotropic Diffusion (AD), the Streamline upwind Petrov- Galerkin (SUGP), the Galerkin least-squares (GLS). In general, it is generally accepted that SUGP does not increase the stability as much as AD or even GLS, but yields higher accuracy and lower computational times.

Crosswind Diffusion. Crosswind Diffusion adds artificial diffusion in the orthogonal direction to the streamlines. For problems that do not involve sharp gradients, the streamline diffusion is often enough to get smooth solutions. In cases where sharp gradients occur, the Crosswind Diffusion is the natural option to reduce spurious oscillations.

In our problem, when no artificial diffusion is employed, the stationary solution is not reached even in the cases we impose the time strict option. At the end of each run, c is almost constant in the whole domain and in some points close to the corners it has no physical sense (negative values and/or higher than 10^{19} mol/m^3). Figure 5 shows the evolution of \bar{c}_1 for $D=10^{-11} \text{ m}^2/\text{s}$ obtained by using the different diffusion

options. For such a small value of D , \bar{c}_1 must reach the value 1 mol/m^3 in stationary regime. In our problem, we have found that the fastest and more realistic solution was obtained by using isotropic diffusion with $\delta_{id}=0.05$. Effectively, Figure 5 shows that isotropic diffusion reaches a stationary solution at $t=10$. The use of the streamline diffusion (artificial diffusion) approximates to the same asymptotic value we obtain for isotropic diffusion. Other choices, such as crosswind diffusion, do not result in stationary solutions.

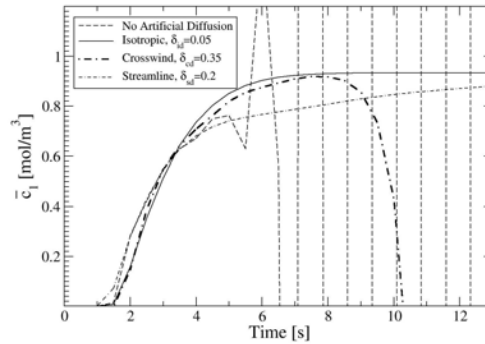


Figure 5: Mean concentration at the exit 1, \bar{c}_1 , as a function of time for different diffusion options. Here, $D=10^{-11} \text{ m}^2/\text{s}$, $\delta_{id}=0.05$ and $Q=0.006 \text{ l/min}$.

Based on these results, we adopted the isotropic diffusion, and all of the results shown here correspond to $\delta_{id}=0.05$. Figure 6 shows the evolution of c until time $t=10\text{s}$, when the solution became stationary (the evolution was continued until $t=20\text{s}$ to monitor the stability of the solution). Notice that at $t=10\text{s}$, a small amount of ink is diffused to the exit #10 and, thus, the concentration of the ink at the boundary #1 is lower than 1 mol/m^3 .

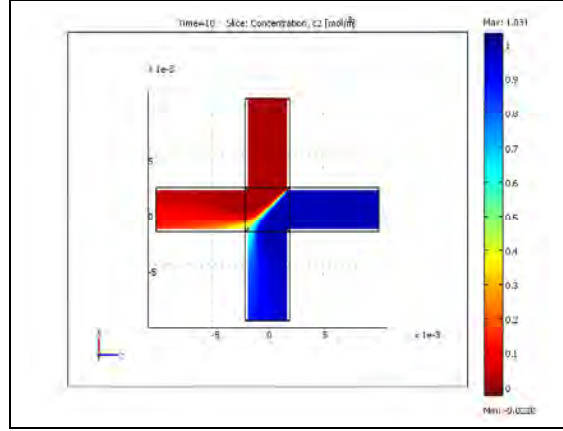
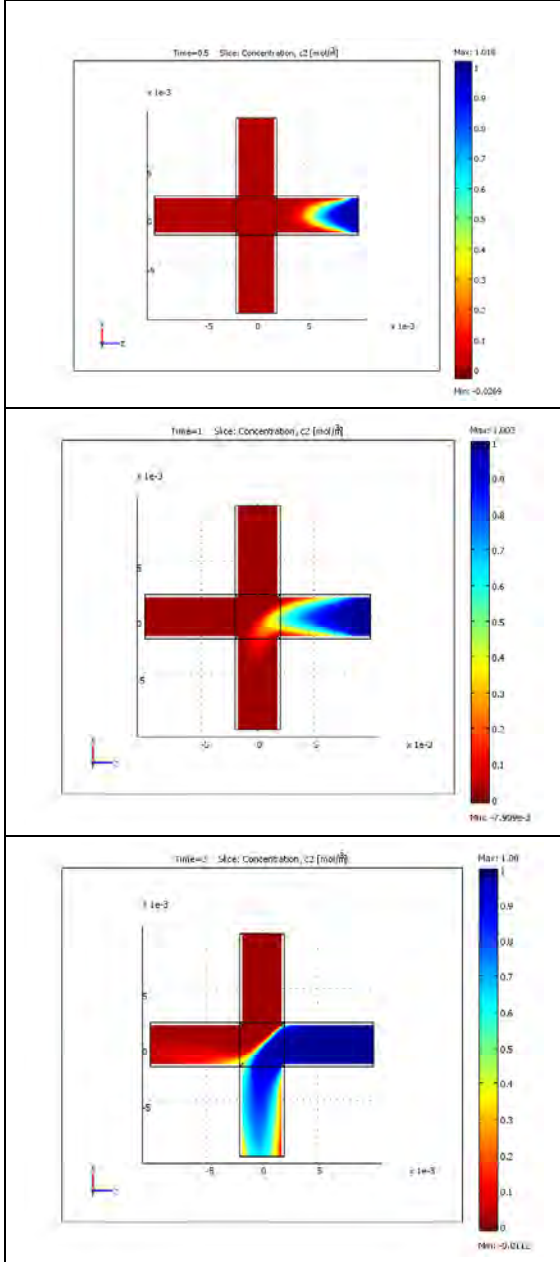


Figure 6: Snapshots of c for $t=0.5, 1, 3$ and 10 seconds. At $t=10$ seconds the solution is steady and identical to the profile $t=20$ seconds (not shown here for brevity). Here, $D=10^{-11} \text{ m}^2/\text{s}$, $\delta_{id}=0.05$ and $Q=0.006 \text{ l/min}$.

Figure 7 shows the dependence of \bar{c}_1 and \bar{c}_{10} as a function of time for $D = 10^{-11} \text{ m}^2/\text{s}$. The asymptotic values for these two quantities are slightly shifted from the theoretical ones, but the error is negligible, about 5%.

We checked that, after the steady state is reached, the sum of both quantities is equal to 1 mol/m^3 , as required for conservation of mass.

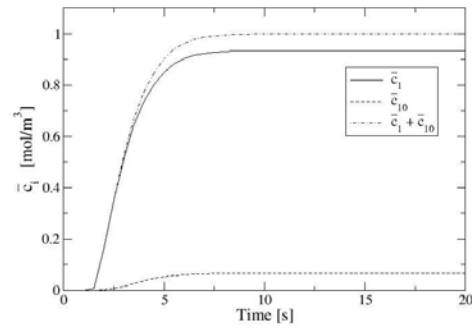


Figure 7: Evolution of the concentration at the exits (boundaries 1 and 10). Here, $D=10^{-11} \text{ m}^2/\text{s}$, $\delta_{id}=0.05$ and $Q=0.006 \text{ l/min}$.

Figure 8 shows the concentration at both exits as a function of D , after the stationary state was reached. We observe that the limits for $D \rightarrow 0$ are $\bar{c}_1, \bar{c}_{10} \rightarrow 0.934, 0.065 \text{ mol/m}^3$ instead of $\bar{c}_1, \bar{c}_{10} \rightarrow 1, 0 \text{ mol/m}^3$. On the other side, the

numerical limits for $D \rightarrow \infty$ are $\bar{c}_1, \bar{c}_{10} \rightarrow 0.521, 478 \text{ mol} / \text{m}^3$ instead of the expected values $\bar{c}_1 = \bar{c}_{10} \rightarrow 0.5 \text{ mol} / \text{m}^3$.

Interestingly, reducing the isotropic diffusion to $\delta_{id}=0.03$, makes the limits to better approach to the theoretical values (see Figure 8).

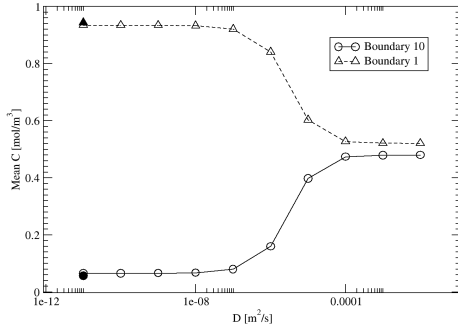


Figure 8: Mean concentration at the exits (boundaries 1 and 10) as a function of D. The isotropic diffusion corresponds to $\delta_{id}=0.05$ (open symbols). The two filled symbols are for $\delta_{id}=0.03$. Here, $Q=0.006$ l/min.

5. Results Analysis

Figure 9 shows the steady state concentration in an experiments with a cross-millichannel at 90 degrees. Intensity of blue color is an indicator of ink concentration.

After the inspection of the experimental image, figure 9, and the numerical simulation, figure 6, we observe similarities and differences in the results. On the one hand, both experiments and simulations predict a small amount of ink crossing the symmetry plane, the ink traveling in the outlet #1 close to the adjacent wall (boundary #12 in figure 9).

On the other side, while experiments do not show an appreciable difference between the concentrations of ink at the exit #10 and the inlet, simulations shows a gradient of concentration in that channel.

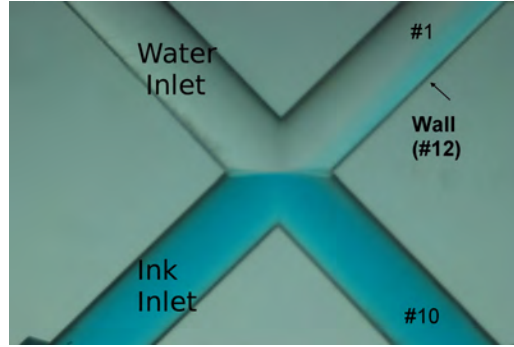


Figure 9: Image of the 90 degrees cross-pipes. Intensity of color ink represents concentration field.

Nevertheless, the numerical results are, in general, in good agreement with experiments. The analysis of figure 9 shows that the concentrations at the outlets are almost 0 and 1 mol/m^3 , while simulations predict exit concentrations to be 0.07 and 0.93 mol/m^3 . We observed that these values are not significantly reduced by reducing D, so we conclude that the small discrepancy between experiments and simulations are due to the artificial diffusion. Effectively, the simulations better approach to the theoretical values of \bar{c} for smaller values of δ_{id} . Unfortunately, the smallest value that gives non-oscillatory solutions is $\delta_{id}=0.03$.

6. Conclusions

A model simulating the hydrodynamics and the convection-diffusion behaviour of a coloured dispersion injected in a X millichannel has been developed in COMSOL Multiphysics.

The model reproduced quantitatively the ratio between the inlet velocity and maximum velocity at the central zone. For the diffusion process, the conservation of mass is satisfied, despite artificial diffusion was employed in order to improve the stability and convergence of the solutions. In conclusion, the numerical simulations qualitatively mimics the general behaviour observed in the experiment. However, we need to reduce artificial diffusion incidence and to optimise meshing in order to achieve outlet concentration values in good agreement with the experimental trials.

7. References

1. Hai Wang and Wei Li, - J. Micromech. Microeng., **17**, 1835–1842 (2007)
2. N. M. Nguyen, S. T. Wereley, Fundamentals and applications of microfluidics, Artech House (2002).
3. J. Bear, Dynamics of fluids in porous media, Elsevier New York (1972).
4. M. Blunt, *Curr. Op. in Coll. and Int. Sci.*, **6**, 197-207 (2001).
5. Comsol Multiphysics Modelling Guide V3.5a (2008)